Mechanism of Domain Closure of Sec7 Domains and Role in BFA Sensitivity†

Louis Renault,‡ Petya Christova,‡,§ Bernard Guibert, Sebastiano Pasqualato, and Jacqueline Cherfils*

Laboratoire d'Enzymologie et Biochimie Structurales, UPR 9063 CNRS, 1, avenue de la Terrasse, 91198 Gif sur Yvette cedex, France

Received December 5, 2001; Revised Manuscript Received January 23, 2002

ABSTRACT: Activation of small G proteins of the Arf family is initiated by guanine nucleotide exchange factors whose catalytic Sec7 domain stimulates the dissociation of the tightly bound GDP nucleotide. The exchange reaction involves distinct sequential steps that can be trapped by the noncompetitive inhibitor brefeldin A, by mutation of an invariant catalytic glutamate, or by removal of guanine nucleotides. Arf-GDP retains most characteristics of its GDP-bound form at the initial low-affinity Arf-GDP−Sec7 step. It then undergoes large conformational changes toward its GTP-bound form at the next step, and eventually dissociates GDP to form a nucleotide-free high-affinity Arf−Sec7 complex at the last step. Thus, Arf proteins evolve through different conformations that must be accommodated by Sec7 domains in the course of the reaction. Here the contribution of the flexibility of Sec7 domains to the exchange reaction was investigated with the crystal structure of the unbound Sec7 domain of yeast Gea2. Comparison with Gea2 in complex with nucleotide-free Arf1Δ17 [Goldberg, J. (1998) *Cell 95*, 237−248] reveals that Arf induces closure of the two subdomains that form the sides of its active site. Several residues that determine sensitivity to brefeldin A are involved in interdomain and local movements, pointing to the importance of the flexibility of Sec7 domains for the inhibition mechanism. Altogether, this suggests a model for the initial steps of the exchange reaction where Arf docks onto the C-terminal domain of the Sec7 domain before closure of the N-terminal domain positions the catalytic glutamate to complete the reaction.

Small G proteins of the Arf[1] family are major regulators of clathrin- and COP1-mediated membrane transport in eukaryotes, with six members grouped in three classes in mammals (*2*). Alternation of GDP and GTP at their nucleotide binding site promotes structural rearrangements which are larger in Arf proteins than in any other small G protein. Structures of GDP-bound Arf proteins (*3*−*6*) show that the switch 1 and switch 2 regions, which bind the γ-phosphate of GTP and are major sites of interaction of G proteins with their partners (reviewed in ref *7*), are remote from GDP, while the binding site for the γ-phosphate is occluded by the aspartate from the DxxGQ motif. The N-terminal amphipathic helix, a myristoylated extension characteristic of Arf proteins, caps a pocket opposite from the nucleotide binding site. In Arf-GTP, the β-strands that connect switch 1 and 2 (called the interswitch hereafter) have translated toward the N-terminal helix pocket (*1*), extruding this helix from the protein core (*8*). Together with the large movement of the switch 1 and 2 regions, this creates a binding site for the γ-phosphate of GTP and, in the cell, couples the activation of Arf by GTP to its recruitment to membranes by its myristoylated helix (reviewed in ref *9*).

GDP-to-GTP exchange is stimulated by ArfGEFs which carry a common catalytic domain of ∼200 amino acids, called the Sec7 domain (reviewed in refs *10* and *11*). More than 12 ArfGEFs have already been identified in mammals, which can be grouped in five subfamilies according to their domain organizations. Their cellular functions in the various aspects of the biogenesis of transport vesicles and the identity of their Arf substrates are not yet fully elucidated. However, most ArfGEFs are active on Arf1 in vitro except the Arf5-specific GBF1 (*12*) and Arf6-specific EFA6 (*13*), while p200/BIGs are inactive on Arf6 (*14*). The regulatory or accessory functions of the domains that flank the catalytic domain are still largely unknown, except for the membrane-targetting pleckstrin homology domains of the ARNO and EFA6 families (reviewed in ref *10*).

Nucleotide exchange catalyzed by Sec7 domains can be schematized according to a general three-step mechanism common to all GEFs (reviewed in ref *15*). It is initiated by the formation of a low-affinity Arf-GDP−Sec7 complex, followed by the dissociation of GDP to form a high-affinity nucleotide-free complex, which is eventually dissociated by GTP to yield active Arf. Valuable insights into this mechanism have been provided by recent structural and biochemical studies. Sec7 domains form an elongated superhelix of helices with a hydrophobic groove that was identified as the

† This work was supported by grants from the Association pour la Recherche contre le Cancer and by the Physique-Chimie du Vivant (CNRS) and Innovations Thérapeutiques (INSERM/CNRS) programs. P.C. was supported by a grant from the CNRS and L.R. by a grant from the EMBO (ALTF 264-1999).

* To whom correspondence should be addressed. Telephone: 33-1-69 82 34 92. Fax: 33-1-69 82 31 29. E-mail: cherfils@lebs.cnrs-gif.fr.

‡ Both authors contributed equally to this work.

§ Present address: Institute of Organic Chemistry, Bulgarian Academy of Sciences, Acad. G. Bonchev St., Bldg 9, Sofia, Bulgaria.

[1] Abbreviations: Arf, ADP ribosylation factor; Arf1Δ17, human Arf1 truncated of the 17 N-terminal residues; ARNO, human Arf nucleotide binding site opener; ARNO-Sec7, Sec7 domain of ARNO; BFA, brefeldin A; BIG, BFA-inhibited GEF; EFA6, exchange factor of Arf6; GBF1, Golgi BFA resistance factor 1; Gea, guanine nucleotide exchange factor for Arf; Gea2-Sec7, Sec7 domain of yeast Gea2; GEF, guanine nucleotide exchange factor; rmsd, root-mean-square deviation.

10.1021/bi012123h CCC: $22.00
Published on Web 02/16/2002

active site (*16*−*18*). The groove is lined on one side by a conserved loop with an invariant glutamate that has been termed the "glutamic finger" for its essential catalytic role (*19*), and by an unusually hydrophobic helix on the other side. The crystal structure of yeast Gea2-Sec7 in complex with human Arf1Δ17 shows how these motifs interact with nucleotide-free Arf and promote its active GTP-bound conformation (*1*). Switch 1 and switch 2 of Arf sit on the groove and the hydrophobic helix of Gea2-Sec7 with which they form an extended interface, while the glutamic finger mimics the charges of the guanine nucleotide phosphates near the phosphate-binding P-loop. An essential finding with this complex is that the two-β-strand interswitch of Arf has translated in the direction of the N-terminal helix pocket, thus elucidating why nucleotide exchange by Sec7 domains requires the concomitant displacement of the myristoylated N-terminal helix by its interaction with membranes (*20*, *21*).

Although no structural information is available on the low-affinity Arf-GDP−Sec7 complex, Sec7 domains are nevertheless unique among GEFs in that this complex can be trapped by mutations of the glutamic finger (*18*, *19*) or by the fungal toxin BFA (*22*), a long-known inhibitor of Golgi traffic (reviewed in ref *23*). In particular, BFA binds at the interface between Arf and BFA-sensitive Sec7 domains and inhibits nucleotide exchange by a noncompetitive mechanism (*22*, *24*, *25*). Not all Sec7 domains are inhibited by BFA. BFA sensitivity is determined by a small number of amino acids in or near the conserved hydrophobic helix, and can be engineered into BFA-insensitive Sec7 domains by introduction of these residues as single mutations, by pairs, or in combination (*22*, *25*, *26*). Remarkably, BFA traps the Arf-GDP−Sec7 complex in the absence of membranes, while mutation of the glutamic finger displaces this complex to membranes (*27*). From the perspective of the nucleotide-free Arf−Sec7 complex structure, these observations indicate that the interswitch is retracted in the Arf-GDP−BFA−Sec7 complex as it is in Arf-GDP, whereas it has undergone its GTP-like translation when the glutamic finger is mutated to a lysine. Thus, the initial docking of Arf-GDP onto the Sec7 domain and the displacement of the interswitch are separable events of the exchange mechanism.

Altogether, these data have established that the biochemical function of Sec7 domains encompasses several aspects, including (1) the initial docking to Arf-GDP, which may be the critical step where specificity is set up (*5*); (2) the displacement of the interswitch region which is necessary to create the binding site for the γ-phosphate of GTP and to stabilize the interaction of Arf with membranes; and (3) the release of the bound nucleotide and the stabilization of the empty nucleotide-binding site promoted by the glutamic finger. Sec7 domains, however, cannot displace the capping N-terminal helix without the assistance of a membrane (*20*, *28*). This mechanism relies on the extreme flexibility and plasticity of Arf proteins along their GDP/GTP cycle, which has been illustrated for Arf1 (*1*, *3*, *4*) and Arf6 (*5*, *8*). As a consequence, Sec7 domains must solve the conflicting requirements of recognizing their substrates in their different conformational states along the reaction pathway.

Here we have investigated the contribution of the flexibility of the Sec7 domain to the exchange reaction with the crystal structure of yeast Gea-Sec7, whose structure in complex with nucleotide-free ArfΔ17 has been determined (*1*). The structure identifies an N-terminal subdomain, which carries the glutamic finger, and a C-terminal subdomain, which encompasses the hydrophobic helix, and shows that these domains behave essentially as rigid bodies that close upon binding of Arf. Residues that are important for the sensitivity of Gea2 to BFA are involved in local conformational changes that support domain closure, suggesting that BFA takes advantage of the flexibility of the Sec7 domain for its inhibitory mechanism. This suggests a model where Arf proteins dock first onto the C-terminal domain, before the glutamic finger domain closes to complete the exchange reaction.

MATERIALS AND METHODS

Protein Expression and Preparation. The Sec7 domain of yeast Gea2 (residues 558−766) was expressed and purified as described in ref *1*. The N-terminal His tag sequence of the pET15b (Novagen) construct was conserved after thrombin cleavage assays failed. Due to cloning artifacts, the protein construct thus possesses an additional N-terminus of 21 amino acids and features the Ile747Val mutation. After purification, the protein was concentrated to 30−40 mg/mL in 20 mM Hepes (pH 7.5), 150 mM KCl, and 1−4 mM DTT, shock-frozen in liquid nitrogen, and stored at −80 °C.

Crystallization. Crystals of the Sec7-Gea2 domain were grown by the hanging drop vapor diffusion method at 20 °C by mixing 1 μL of the stored protein solution with 1 μL of the reservoir solution. The largest crystals were obtained with a reservoir solution containing 1.4 M ammonium sulfate, 0.1 M sodium acetate, or sodium citrate (pH 5.0) using microseeding. Crystals grew within 3 weeks to a size of ∼200 μm × 50 μm × 30 μm. Data collections were performed at 100 K with crystals flash-cooled in liquid ethane after soaking for few seconds in a cryoprotectant solution consisting of 35% (v/v) glycerol and 2.25 M ammonium sulfate, 0.1 M sodium acetate or sodium citrate (pH 5.0), and 0.15 M KCl.

Data Collection and Processing. The crystals belong to space group *C*2 with two molecules in the asymmetric unit with the following average unit cell dimensions: $a = 125.05$ Å, $b = 75.88$ Å, $c = 76.20$ Å, and $\beta = 105.37°$. High-resolution data sets were collected at LURE (Orsay, France) on the DW32 beamline to a resolution limit of 2.4 Å, and at DESY (Hamburg, Germany) on the MPG/GBF wiggler beamline BW6/DORIS to a resolution limit of 1.9 Å. The diffraction frames were processed with DENZO and reduced with SCALEPACK (*29*). The two high-resolution data sets were merged to improve the redundancy and completeness, especially to recover overloaded low-resolution reflections in the DESY data set. A summary of the data sets and the processing statistics is given in Table 1.

Structure Determination and Refinement. The structure was determined by the molecular replacement method using AMoRe (*30*) with Gea2-Sec7 determined in complex with Arf1Δ17 (*1*) as a search model. This resulted in a correlation of amplitudes of 52.4% and a crystallographic R_{factor} of 45.7% using the data set collected at LURE with a resolution range from 20 to 4.0 Å. Seven percent of the reflections were set aside for an R_{free} test before initiating any refinement. The program O (*31*) was used for model building, and CNS (version 1.1) (*32*) with bulk solvent correction was used for

Table 1: Data Collection and Refinement Statistics

	DW32 at LURE	BW6 at DESY	merge of the two data sets
wavelength (Å)	0.948	1.050	
*C*2 unit cell parameters	$a = 125.27$ Å	$a = 125.03$ Å	$a = 125.05$ Å
	$b = 75.56$ Å	$b = 75.86$ Å	$b = 75.88$ Å
	$c = 76.33$ Å	$c = 76.22$ Å	$c = 76.20$ Å
	$\beta = 105.30°$	$\beta = 105.41°$	$\beta = 105.37°$
mosaicity in Denzo (deg)	1.00	0.50	
resolution range (Å)	20.1−2.39	25.0−1.93	25.0−1.93
last resolution shell (Å)	2.43−2.39	1.97−1.93	1.97−1.93
rotation range (deg)	220	117	
no. of unique reflections	27036	52428	52653
multiplicity (last shell)	3.5 (3.2)	3.0 (2.1)	4.6 (2.1)
completeness (%) (last shell)	98.9 (97.9)	96.6 (94.3)	97.0 (94.4)
R_{sym}[a] (last shell)	0.058 (0.261)	0.042 (0.327)	0.080 (0.326)
I/σ (last shell)	18.6 (4.3)	21.7 (2.6)	14.6 (2.7)

Refinement	
resolution (Å) (last shell)	25.0−1.93 (1.97−1.93)
no. of reflections (work set/test set)	46579/3709
no. of protein atoms	3412
no. of solvent atoms	217
R_{factor}[b] (last shell)	0.214 (0.276)
R_{free}[c] (last shell)	0.228 (0.298)
rmsd[d] for bond lengths (Å)	0.006
rmsd[d] for bond angles (deg)	1.4

[a] $R_{sym} = \sum_h \sum_i |I_{h,i} - \langle I_h \rangle| / \sum_h \sum_i I_{h,i}$. [b] $R_{factor} = \sum_h |F_o - F_c| / \sum F_o$ (working set, no σ cutoff applied). [c] R_{free} is the R_{factor} based on 7% of the data excluded from the refinement. [d] Root-mean-square deviation (rmsd) from target geometries.

automated refinement. Noncrystallographic restraints were only used in the early stages of the refinement. The final model contains residues 558−759 from the Sec7 domain with nine additional N-terminal residues from the plasmid (added sequence GLVPRGSHM) for each of the two molecules of the asymmetric unit; 86.9% of the residues are in the most favored region of the Ramachandran diagram, and two residues in a poorly defined region are in the disallowed region. The two molecules in the asymmetric unit differ slightly in the relative orientations of their N- and C-terminal subdomains (see the Results) such that the rmsd is ≈0.3 Å between the subdomains and ≈0.9 Å for the entire domain. Coordinates have been deposited with the Protein Data Bank as entry 1KU1.

Model Depiction. Superimpositions were produced with TURBO (http://afmb.cnrs-mrs.fr/subjects/turbo) and the CCP4 programs suite (*33*). Domain closure angles were computed with DOMOV (http://bioinfo1.mbfys.lu.se/cgi-bin/Domov/domov.cgi). Figures were drawn with Molscript (*34*) and Raster3D (*35*).

RESULTS

Comparison of Unbound and Complexed Gea2. The crystal structure of the Sec7 domain of yeast Gea2 was determined at 1.9 Å resolution by molecular replacement. Its overall superposition to Gea2 bound to nucleotide-free Arf1Δ17 (*1*) yields an rmsd of 0.9 Å, a value that drops to 0.4 and 0.35 Å when the two halves of Gea2-Sec7 that form the sides of the catalytic groove are fitted individually, thus defining two subdomains (termed the N-terminal and C-terminal domains hereafter) (Figure 1a,b). The N-terminal domain comprises helices α1−α5, the Glu finger loop, and the N-terminal half of helix α7, while the C-terminus of helix α7 is associated with helix α6 (which precedes the Glu finger loop) and helices α8−α10 to form the C-terminal domain (Figure 1c). Thus, the N- and C-terminal domains are displaced essentially as rigid bodies as Gea2-Sec7 binds to Arf and catalyzes nucleotide exchange. The partial association of helix α7 with each domain reflects its change from a straight to a bent conformation upon binding to Arf, with an increase of 0.7 Å in the intrahelical hydrogen bond at Arg^{660}−Ala^{664} which nevertherless preserves the helical conformation (Figure 1d).

The movement has an amplitude of ≈9−10° with three hinges located at Phe^{631} in the α5−α6 loop, Lys^{648} between helix α6 and the beginning of the Glu finger loop, and Phe^{665} in the middle of helix α7 (first molecule of the asymmetric unit). Lys^{648} and Phe^{665} define a rotation axis for the Glu finger loop, while rotation on a single hinge of the remaining part of the N-terminal domain requires that it leans against the Glu finger loop. Domain rotation in the Gea2−Arf complex results in a closure of the catalytic hydrophobic groove by 3.2 Å, as estimated by the Cα−Cα distance between the Glu finger (Glu^{654}) and Met^{707} in the hydrophobic helix. A somewhat larger displacement, due to an additional point rotation of ≈4−5° centered near Phe^{631}, is observed in the second Gea2 molecule in the asymmetric unit, which has an otherwise similar subdomain separation (0.4 Å larger than in the first molecule) and local changes.

Although domain closure narrows the catalytic groove, rearrangements of amino acids at the domain interface are limited to Tyr^{703} [corresponding to Tyr^{146} in Gea2-Arf numbering (*1*) and Phe^{190} in ARNO (*16*, *17*)] (Figure 2a). The hydroxyl of Tyr^{703} interacts with the main chain of Glu^{659} from helix α7 in unbound Gea2-Sec7, but would clash with this helix in its closed Arf-bound conformation. Accordingly, the side chain of Tyr^{703} is rotated in bound Gea2, where it forms a hydrogen bond with the hydroxyl of Ser^{655} next to the Glu^{654} finger and with Trp^{78} from switch 2 of Arf (Figure 2a). Unbound Gea2 and complexed Gea2 also differ at the loop that connects helices α8 and α9 in the C-terminal domain (Figure 2b), which is involved in binding switch 1 of Arf in

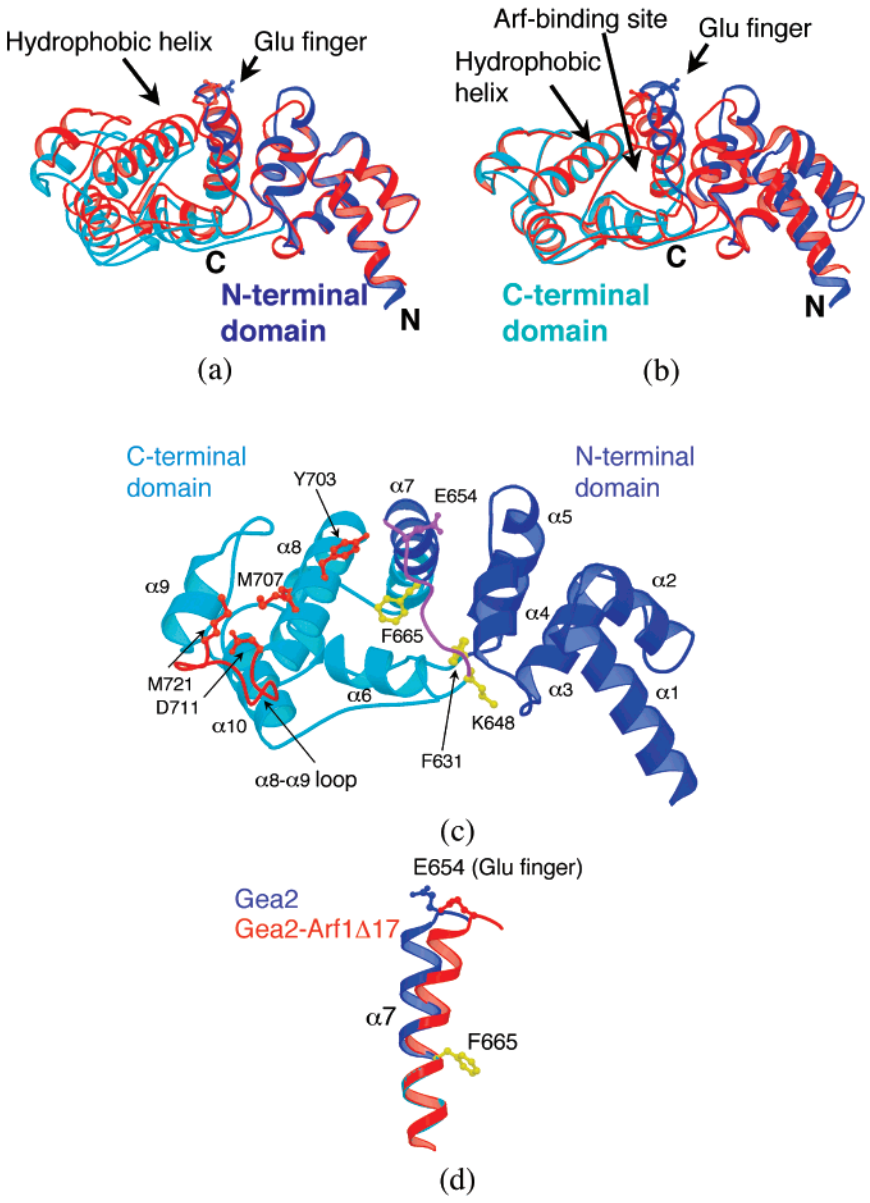

FIGURE 1: Domain closure of Gea2. (a) Superposition of the N-terminal domains from unbound and Arf-bound Gea2. The N- and C-terminal subdomains of unbound Gea2 are in dark blue and cyan, respectively. Gea2 in the nucleotide-free complex with Arf1Δ17 (*1*) is in red. (b) Superposition of the C-terminal domains from unbound and Arf-bound Gea2. Colors are as in panel a. (c) Structure of unbound Gea2. The glutamic finger loop is in violet and moves with the N-terminus domain. Hinge residues are in yellow. Residues important for the sensitivity to BFA and the α8−α9 loop are in red. The Arf binding site is at the interface between the N- and C-terminal domains and encompasses helices α7−α9 and the Glu finger loop (*1*). (d) Comparison of helix α7 in unbound Gea2 (straight) and in the Gea2−Arf1Δ17 complex (bent). Domain colors are as in panel a.

the nucleotide-free complex. The movement amounts to 3 Å with end points at Asp[711] and Met[721], which are connected through a hydrogen bond from the carboxylate of Asp[711] to the main chain of Met[721].

Comparison of Gea2 to ARNO. Superposition of the structure of unbound ARNO-Sec7 (*16*, *17*), a mammalian small ArfGEF, with that of unbound Gea2-Sec7 delineates subdomains that are equivalent to those identified between bound and unbound Gea2 (Figure 3). The angular separation between the N- and C-terminal domains is ≈6° larger in ARNO than in unbound Gea2, with a Cα−Cα distance between the Glu finger (Glu[156]) and Met[194] in the hydrophobic helix that is 2 Å larger than in unbound Gea2, and 5.2 Å larger than in the Gea2−Arf1Δ17 complex. However, the hinge residues in ARNO (Phe[134], Ser[150], and Phe[167]) superimpose with those of Gea2, suggesting that ARNO is likely to undergo domain closure of a nature similar to that of Gea2, but larger in amplitude. The major structural difference between Gea2 and ARNO at their domain interface is located in the hydrophobic motif at Tyr[703], which is replaced in ARNO with Phe[190] and cannot form an internal hydrogen bond with helix α7 (Figure 2a). Phe[190] also cannot form a hydrogen bond with switch 2 of Arf as observed between between Tyr[703] and Trp[78] in the Gea2−Arf1Δ17 complex (*1*). Thus, the conservation of Tyr and/or Phe residues at this location suggests that their aromatic nature is required for them to act as spacers between the N- and C-terminal domains, as well as to insert between switch 1 and switch 2. The hydroxyl of Tyr, on the other hand, may restrict the interdomain motions and spacing of Gea2, which may have implications for the specific recognition of Arf substrates (see the Discussion). Other structural differences

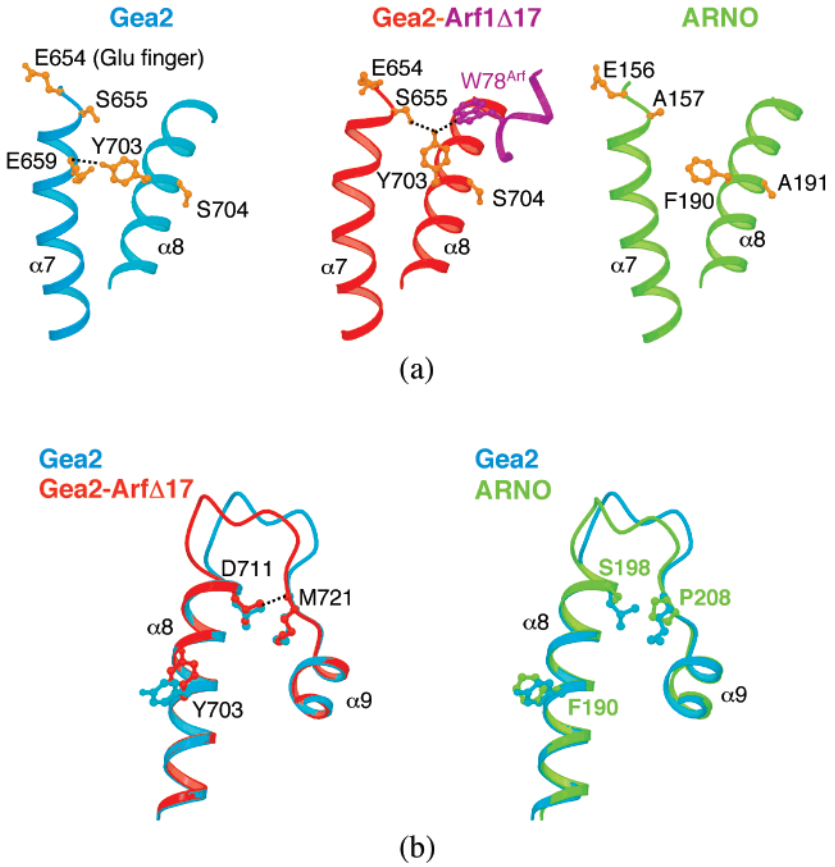

FIGURE 2: Conformation of BFA-sensitive residues. (a) Tyr/Ser (BFA-sensitive) vs Phe/Ala (BFA-resistant) sequences in helix α8. Interactions of helix α7 with helix α8 are shown for unbound Gea2 (blue, left), the Gea2−Arf1Δ17 complex (*1*) (Gea2 in red and Arf1Δ17 in violet, middle) and ARNO (*16*) (green, right). Hydrogen bonds are shown as dotted lines. (b) Asp/Met (BFA-sensitive) vs Ser/Pro (BFA-resistant) sequences in the α8−α9 loop. Superpositions are shown between unbound and bound Gea2 (left) and between unbound Gea2 and ARNO (right).

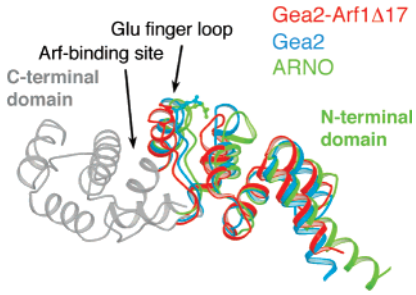

FIGURE 3: Open conformation of ARNO. Superposition of ARNO (green), unbound Gea2 (blue), and the Gea2−Arf1Δ17 complex (red) based on their C-terminal domains. Only the C-terminal domain of ARNO (gray) is shown for clarity (rmsd of 0.5 Å between ARNO and Gea2).

between ARNO and Gea2 are located at the switch 1-binding α8−α9 loop, the end points of which are equivalent to those found by comparing this loop between unbound and complexed Gea2 (Figure 2b). However, the hydrogen bond between Asp^{711} and Met^{721} in Gea2 cannot be formed between Ser^{198} and Pro^{208} in ARNO (Figure 2b). Strikingly, these residues as well as the Tyr/Phe substitution in the hydrophobic motif have been identified as key determinants of the sensitivity to BFA (*22*, *25*, *26*) (see below).

DISCUSSION

Recognition of Arf-GDP by the Open Conformation of Sec7 Domains. The crystal structure of unbound Gea2-Sec7 and its comparison to Gea2 bound to nucleotide-free Arf1Δ17 (*1*) show that the N-terminal and C-terminal domains, which contain the Glu finger loop and the hydrophobic helix, respectively, undergo essentially rigid-body closure induced by binding of Arf. It is the first example of a helical GEF characterized in both its bound and unbound conformations and the first demonstration that the large conformational changes that characterize the activation of small G proteins are accompanied by concomitant conformational changes of a GEF, although to a significantly lower amplitude. A similar yet slightly more open conformation involving the same structural domains is also observed in the previously reported structure of unbound ARNO-Sec7 (*16*). This suggests that domain closure may be a general feature of the mechanism of Sec7 domains. This is supported by NMR studies of Cytohesin 1 (*18*), which report chemical shifts near helix α6 upon binding to Arf, a region that does not contact Arf in the complex (*1*) but is close to the interdomain hinges (this study). Furthermore, differences between the two unbound Gea2-Sec7 molecules in the crystal suggest that domain closure is facilitated by intrinsic flexibility between the N- and C-terminal Sec7 subdomains. Two hinge residues, Phe^{631} and Phe^{655} in Gea2, are highly conserved in most Sec7 domains. In particular, Phe^{655} corresponds to the helical hinge of helix α7 in Arf-bound Gea2, suggesting that this helix might be straight in all unbound ArfGEFs, and adopt a bent conformation in their Arf-bound form. The resulting strain in Arf-bound Sec7

domains might store elastic energy (reviewed in ref *36*) that could be used to release nucleotide-bound Arf from the complex.

Although both the N- and C-terminal domains are tightly bound to Arf in the nucleotide-free complex, mutation of the Glu finger to Lys or Ala does not impair the ability of Sec7 domains to bind to Arf-GDP (*18*, *19*), making it unlikely that this residue interacts with Arf-GDP at the docking stage. This view is strengthened by the observation that all the residues that affect the sensitivity of Sec7 domains to BFA, a drug that traps Arf essentially in its GDP conformation (*27*), are located in the C-terminal domain (*22*, *26*), whereas mutation of the Glu finger in the BFA-sensitive quadruple mutant of ARNO has no effect on its ability to form the abortive Arf-GDP−BFA−Sec7 complex (*25*). Since the C-terminal domain interacts extensively with the switch 2 region of Arf, we propose that an early event of the formation of the Arf-GDP−Sec7 interface is the anchoring of switch 2 onto the C-terminal region, and that the open conformation of the Sec7 domains contributes to exclude the catalytic glutamate from the vicinity of the nucleotide. Yet, if we assume that switch 2 interacts with the C-terminal domain as it does in the nucleotide-free complex, none of the nucleotide-bound structures of Arf1 or Arf6 would fit without a clash at switch 1 or would exclude the glutamic finger from the nucleotide binding site. This suggests that either the orientation of Arf-GDP relative to the C-terminal domain is different at the docking step from that in the nucleotide-free complex or Arf proteins take advantage of their giving plasticity to rotate their switch 2 portions to an angular range wider than that characterized in the GDP/GTP structural cycles of Arf1 (*1*, *3*, *4*) and Arf6 (*5*, *8*).

Specificity of GEFs for individual, or classes of, small G proteins has been reported for several ArfGEFs (reviewed in ref *10*) as well as for GEFs for other families of small G proteins. To be effective in the cells, structural interactions that determine specificity are likely to form before GDP has dissociated from the GEF−G protein complex, since cellular conditions, including the higher abundance of free GTP, tend to favor binding of GTP to the nucleotide-free complex. In the case of Arf proteins and their ArfGEFs, a mechanism excluding the Glu finger from the GDP binding site in the docking Arf-GDP−GEF complex would fulfill this requirement. We propose in addition that the width of the unbound catalytic groove, which can vary between individual Sec7 domains as shown between ARNO and Gea2, is used as a sensor of the relative positions and flexibilities of switches 1 and 2 of individual members of the Arf family in their GDP-bound forms. Differences in these structural parameters between related small G proteins have been observed between Arf1 and Arf6 (*3*, *5*) and in other small G proteins such as the Ras/Rap family (*37*, *38*), where they may contribute to determining specific protein−protein interactions. Interestingly, GEFs for Ras (cdc25 domain) and for Rho (Dbl homology domain) have recently been suggested to initiate nucleotide exchange through their docking at switch 2 (*39*, *40*), and to involve domain motion in the case of RhoGEFs (*40*), pointing to the possibility that this is a general mechanism of helical GEFs for the recognition of their GDP-bound substrates. The β-propeller structure of RCC1, a GEF for Ran that has been determined alone and in complex with nucleotide-free Ran, departs from this model as it behaves as a rigid scaffold with limited local rearrangements (*41*).

Flexibility of Sec7 Domains and Sensitivity to BFA. ARNO and Gea2, whose unbound structures are compared here, are representative members of BFA-resistant and BFA-sensitive ArfGEFs, respectively. Sensitivity to BFA can be engineered into ARNO by mutation of Phe^{190} and Ala^{191} to Tyr and Ser, respectively, in the hydrophobic helix and/or Ser^{198} and Pro^{208} to Asp and Met, respectively, at the end points of the α8−α9 loop (*22*, *25*), which correspond to sequences conserved in BFA-sensitive ArfGEFs such as yeast Gea2 (Tyr^{703}, Ser^{704}, Asp^{711}, and Met^{721}) (*22*) or mammalian BIGs/p200 (*24*). Ser/Asp or Pro/Met single mutations are also sufficient to confer BFA sensitivity to Cytohesin1, a close homologue of ARNO (*26*). The Ala/Ser substitution has not been characterized as a single mutation, but it is buried in all structures of Sec7 domains and is likely not involved in their sensitivity to BFA. Here we have shown that Tyr^{703}, Asp^{711}, and Met^{721} form two additional internal hydrogen bonds in unbound Gea2 as compared to Phe^{190}, Ser^{198}, and Pro^{208} in ARNO, and that these residues are involved in conformational flexibility of the Sec7 domain on going from the open to the closed conformation. Thus, both their potential ability to form hydrogen bonds with BFA and their contribution to the conformation and flexibility of unbound Sec7 domains may contribute to the sensitivity to BFA. In particular, different flexibilities at the α8−α9 loop may be critical for the Arf−Sec7 interface to allow entry of BFA and/or to accommodate the drug at the Arf−Sec7 interface. The presence of these three residues is not sufficient, however, for the BFA-sensitive quadruple mutant of ARNO to form an inhibited complex with Arf6-GDP in the presence of BFA (unpublished results; E. Macia and M. Franco, personal communication). This may result from differences between Arf1 and Arf6 in the flexibilities of their switch 2 regions and/or the conformations of their switch 1 regions as identified from the crystal structures of their GDP-bound forms (*3*, *5*). Altogether, this suggests that sensitivity to BFA is determined by both the ArfGEF and Arf proteins, and that their flexibility is one of its key features.

Domain Closure and the Glutamic Finger. We hypothesize from this study that the glutamic finger is remote from the nucleotide binding site in the Arf-GDP−Sec7 docking complex, and that both domain closure of the Sec7 domain and conformational changes in Arf are required for its interaction with the conserved lysine from the P-loop in the nucleotide-free complex and its mimicry of the GDP β-phosphate (*1*). As a consequence of domain closure, the glutamic finger, through its negative electrostatic field, could successively destabilize different interactions along its trajectory, including the interactions of negatively charged residues from Arf as well as those of the phosphate of the GDP nucleotide. In this regard, examination of the nucleotide-free complex reveals an essential role of Asp^{26} in the GLDAAGKT motif of the P-loop of Arf. This residue forms a salt bridge with Arg^{99} in helix α3 in nucleotide-bound Arf1 (Figure 4a), and an additional ion pair with Arg^{75} in Arf1-GTP. Remarkably, Asp^{26} moves by more than 4 Å in nucleotide-free Arf1 such that it binds to Asn^{126} and Lys^{127} from the base binding sequence NKQD, while a hydrogen bond to Gly^{29} from the P-loop adds a turn to helix α1 (Figure 4b) (*1*). Superposition of GDP-bound Arf with the nucleotide-

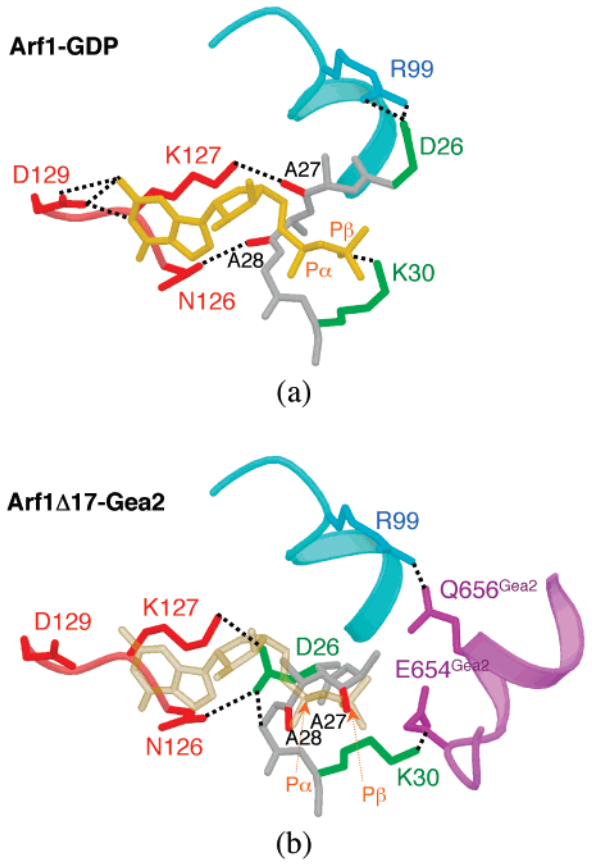

FIGURE 4: Proposed role for Asp[26] and the Glu finger in the dissociation of GDP. (a) Interaction of Asp[26] in GDP-bound Arf1 (*3*). The P-loop is in gray with the carbonyls of Ala[27] and Ala[28] shown in red, helix α3 in cyan, and the GDP nucleotide in yellow. Residues from the NKQD motif are in red. (b) Interactions of Asp[26] in the nucleotide-free Arf1Δ17−Gea2 complex (*1*). The GDP nucleotide from Arf1-GDP is superimposed in transparency. The Glu[654] finger and helix α7 from Gea2 are in violet.

free complex reveals that these interactions distort the P-loop such that the carbonyls of Ala[28] and Ala[27] mimic the α- and *β*-phosphates of GDP, respectively (Figure 4b). Such an elaborate function of Asp[26], combining distortion of the P-loop with stabilization of the nucleotide-free binding site, suggests that its conformational change is a previously unappreciated contribution of the Sec7 domain, rather than a consequence of nucleotide release as initially proposed (*1*). The negative electrostatic field of the Glu finger would be well-suited to triggering the displacement of Asp[26] which would then drive the distortion of the P-loop. The steric conflict of the distorted P-loop with the α- and *β*-phosphates of GDP in coordination with their destabilization by charge repulsion from the Glu finger would eventually yield the dissociation of GDP. The resulting empty nucleotide-binding site must then be stabilized, which is probably the role of the numerous interactions observed in the nucleotide-free complex [Asp[26] with the base-binding residues, Glu[654] finger (Gea2) with Lys[30] from the P-loop of Arf, and Gln[656] (Gea2) with Arg[99] in helix α3 of Arf].

In conclusion, our structural study refines the current model of the multistep nucleotide exchange reaction catalyzed by ArfGEFs, establishing domain closure and local conformational changes of the Sec7 domain as components of the mechanism. Together with previous structural and biochemical studies, this suggests that the reaction is initiated by anchoring of Arf-GDP on the C-terminal domain excluding the Glu finger, which is subsequently positioned by domain closure to dissociate GDP and stabilize the nucleotide-free complex. Yet the conformation of switch 2 at the docking complex, the Sec7−Arf interactions that trigger the unfolding of switch 1, and those that drive the movement of the interswitch still remain to be established to complete the structural description of the reaction pathway.

ACKNOWLEDGMENT

We thank J. Goldberg (Memorial Sloan-Kettering Cancer Center, New York, NY) for the gift of the His-tagged Gea2-Sec7 plasmid, B. Olofsson (LEBS, Gif-sur-Yvette, France) for help with the Gea2 plasmid, and the staff at the LURE (Orsay, France) and DESY (Hamburg, Germany) synchrotrons for making beamlines available to us.

REFERENCES

1. Goldberg, J. (1998) *Cell 95*, 237−248.
2. Chavrier, P., and Goud, B. (1999) *Curr. Opin. Cell Biol. 11*, 466−475.
3. Amor, J. C., Harrison, D. H., Kahn, R. A., and Ringe, D. (1994) *Nature 372*, 704−708.
4. Greasley, S. E., Jhoti, H., Teahan, C., Solari, R., Fensome, A., Thomas, G. M., Cockcroft, S., and Bax, B. (1995) *Nat. Struct. Biol. 2*, 797−806.
5. Menetrey, J., Macia, E., Pasqualato, S., Franco, M., and Cherfils, J. (2000) *Nat. Struct. Biol. 7*, 466−469.
6. Amor, J. C., Horton, J. R., Zhu, X., Wang, Y., Sullards, C., Ringe, D., Cheng, X., and Kahn, R. A. (2001) *J. Biol. Chem. 276*, 42477−42484.
7. Vetter, I. R., and Wittinghofer, A. (2001) *Science 294*, 1299−1304.
8. Pasqualato, S., Menetrey, J., Franco, M., and Cherfils, J. (2001) *EMBO Rep. 2*, 234−238.
9. Roth, M. G. (1999) *Trends Cell Biol. 9*, 174−179.
10. Jackson, C. L., and Casanova, J. E. (2000) *Trends Cell Biol. 10*, 60−67.
11. Donaldson, J. G., and Jackson, C. L. (2000) *Curr. Opin. Cell Biol. 12*, 475−482.
12. Claude, A., Zhao, B. P., Kuziemsky, C. E., Dahan, S., Berger, S. J., Yan, J. P., Armold, A. D., Sullivan, E. M., and Melancon, P. (1999) *J. Cell Biol. 146*, 71−84.
13. Franco, M., Peters, P. J., Boretto, J., van Donselaar, E., Neri, A., D'Souza-Schorey, C., and Chavrier, P. (1999) *EMBO J. 18*, 1480−1491.
14. Morinaga, N., Adamik, R., Moss, J., and Vaughan, M. (1999) *J. Biol. Chem. 274*, 17417−17423.
15. Cherfils, J., and Chardin, P. (1999) *Trends Biochem. Sci. 24*, 306−311.
16. Cherfils, J., Menetrey, J., Mathieu, M., Le Bras, G., Robineau, S., Beraud-Dufour, S., Antonny, B., and Chardin, P. (1998) *Nature 392*, 101−105.
17. Mossessova, E., Gulbis, J. M., and Goldberg, J. (1998) *Cell 92*, 415−423.
18. Betz, S. F., Schnuchel, A., Wang, H., Olejniczak, E. T., Meadows, R. P., Lipsky, B. P., Harris, E. A., Staunton, D. E., and Fesik, S. W. (1998) *Proc. Natl. Acad. Sci. U.S.A. 95*, 7909−7914.
19. Beraud-Dufour, S., Robineau, S., Chardin, P., Paris, S., Chabre, M., Cherfils, J., and Antonny, B. (1998) *EMBO J. 17*, 3651−3659.
20. Franco, M., Chardin, P., Chabre, M., and Paris, S. (1996) *J. Biol. Chem. 271*, 1573−1578.
21. Chardin, P., Paris, S., Antonny, B., Robineau, S., Beraud-Dufour, S., Jackson, C. L., and Chabre, M. (1996) *Nature 384*, 481−484.
22. Peyroche, A., Antonny, B., Robineau, S., Acker, J., Cherfils, J., and Jackson, C. L. (1999) *Mol. Cell 3*, 275−285.
23. Jackson, C. L. (2000) *Subcell. Biochem. 34*, 233−272.

24. Mansour, S. J., Skaug, J., Zhao, X. H., Giordano, J., Scherer, S. W., and Melancon, P. (1999) *Proc. Natl. Acad. Sci. U.S.A. 96*, 7968−7973.
25. Robineau, S., Chabre, M., and Antonny, B. (2000) *Proc. Natl. Acad. Sci. U.S.A. 97*, 9913−9918.
26. Sata, M., Moss, J., and Vaughan, M. (1999) *Proc. Natl. Acad. Sci. U.S.A. 96*, 2752−2757.
27. Béraud-Dufour, S., Paris, S., Chabre, M., and Antonny, B. (1999) *J. Biol. Chem. 274*, 37629−37636.
28. Antonny, B., Beraud-Dufour, S., Chardin, P., and Chabre, M. (1997) *Biochemistry 36*, 4675−4684.
29. Otwinowski, Z. (1993) *CCP4 Study Weekend: Data Collection and Processing*, pp 56−62, Daresbury Laboratory, Warrington, U.K.
30. Navaza, J. (1994) *Acta Crystallogr. A50*, 157−163.
31. Jones, T. A., and Kjeldgaard, M. (1997) *Methods Enzymol. 277*, 173−208.
32. Brunger, A. T., Adams, P. D., Clore, G. M., DeLano, W. L., Gros, P., Grosse-Kunstleve, R. W., Jiang, J. S., Kuszewski, J., Nilges, M., Pannu, N. S., Read, R. J., Rice, L. M., Simonson, T., and Warren, G. L. (1998) *Acta Crystallogr. D54*, 905−921.
33. Collaborative Computational Project No. 4 (1994) *Acta Crystallogr. D50*, 760−763.
34. Kraulis, P. J. (1991) *J. Appl. Crystallogr. 24*, 946−950.
35. Merrit, E. A., and Bacon, D. J. (1997) *Methods Enzymol. 277*, 505−524.
36. Hayward, S. (1999) *Proteins 36*, 425−435.
37. de Vos, A. M., Tong, L., Milburn, M. V., Matias, P. M., Jancarik, J., Noguchi, S., Nishimura, S., Miura, K., Ohtsuka, E., and Kim, S. H. (1988) *Science 239*, 888−893.
38. Cherfils, J., Menetrey, J., Le Bras, G., Janoueix-Lerosey, I., de Gunzburg, J., Garel, J. R., and Auzat, I. (1997) *EMBO J. 16*, 5582−5591.
39. Hall, B. E., Yang, S. S., Boriack-Sjodin, P. A., Kuriyan, J., and Bar-Sagi, D. (2001) *J. Biol. Chem. 276*, 27629−27637.
40. Cherfils, J. (2001) *FEBS Lett. 507*, 280−284.
41. Renault, L., Kuhlmann, J., Henkel, A., and Wittinghofer, A. (2001) *Cell 105*, 245−255.

BI012123H